

Impact of dimensionality and confinement on the electronic properties of mercury chalcogenides nanocrystals

Charlie Gréboval¹, Eva Izquierdo², Clément Livache^{1,2}, Bertille Martinez^{1,2}, Marion Dufour², Nicolas Goubet^{1,2}, Nicolas Moghaddam², Junling Qu¹, Audrey Chu¹, Julien Ramade¹, Hervé Aubin², Hervé Cruguel¹, Mathieu Silly³, Emmanuel Lhuillier^{1*}, Sandrine Ithurria²

¹Sorbonne Université, CNRS, Institut des NanoSciences de Paris, INSP, F-75005 Paris, France

²Laboratoire de Physique et d'Etude des Matériaux, ESPCI-Paris, PSL Research University, Sorbonne Université UPMC Univ Paris 06, CNRS, 10 rue Vauquelin 75005 Paris, France.

³Synchrotron-SOLEIL, Saint-Aubin, BP48, F91192 Gif sur Yvette Cedex, France

To whom correspondence should be sent: el@insp.upmc.fr

Table of content

1. Material characterization	2
2. Photoemission signal.....	5
2.1. Core level analysis	5
2.2. Pump probe photoemission	6
3. Experimental setup used for transport measurements	7
3.1. Field effect transistor measurements	7
3.2. Time-resolved photoresponse.....	7
3.3. Noise measurement	8
4. References.....	8

1. Material characterization

TEM image of HgTe/CdS reveals that they present enrolled 2D aspect, see Figure S 1. In Figure S 2, high resolution image are provided

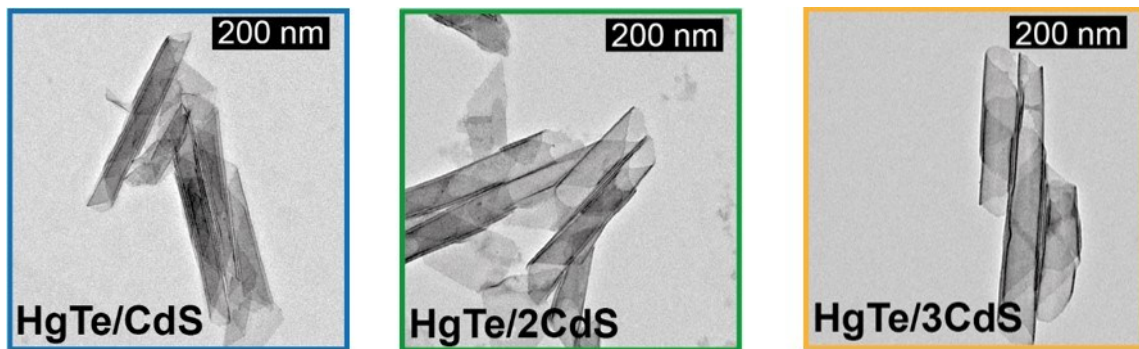


Figure S 1 TEM image of HgTe/CdS NPLs (left), HgTe/2CdS NPLs (middle) and HgTe/3CdS NPLs (right)

The crystalline nature of the final core shell object can be confirmed by high resolution TEM imaging, see Figure S 2 and X-ray diffraction, see Figure S 3

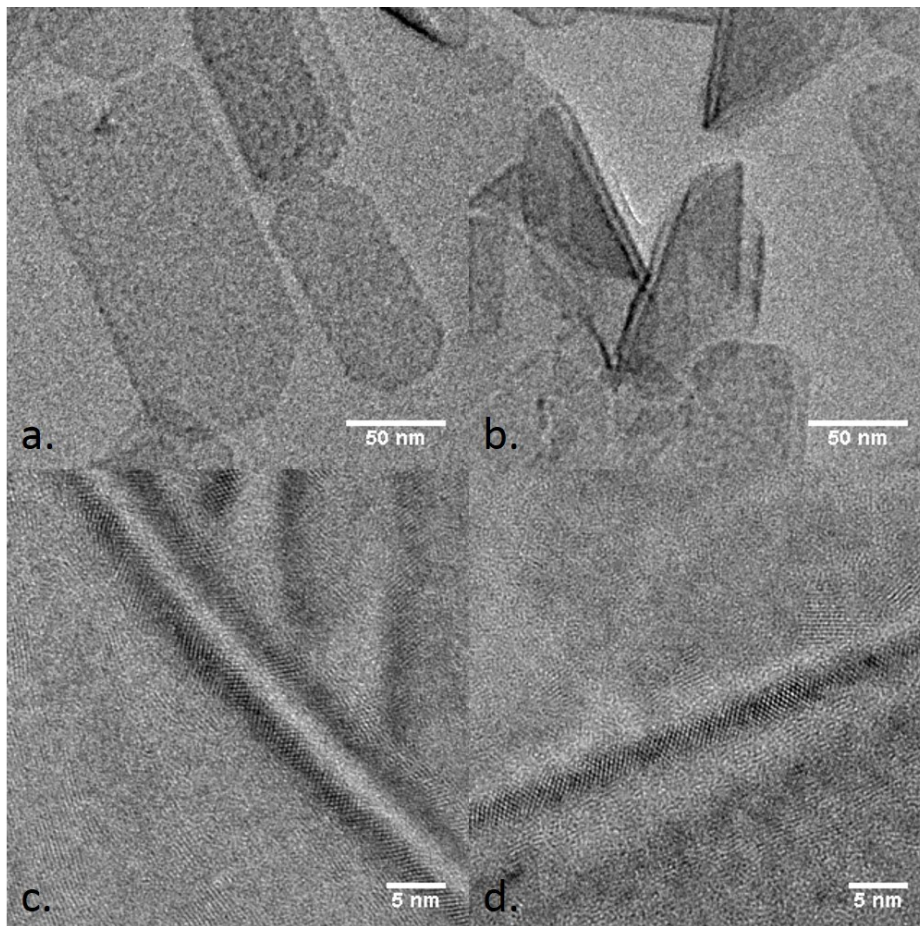


Figure S 2 High resolution TEM of HgTe/3CdS NPL

The growth of the CdS shell is expected to lead to some strain on the HgTe core due to the material lattice mismatch and as suggested by the enrolment of the NPL. X-ray diffraction confirms this prediction. While the cation exchange step from CdTe to HgTe lets the diffractogram mostly unaffected, see Figure S 3. The growth of the CdS shell (0.58 nm for CdS lattice parameter on the top of HgTe with a 0.646 nm lattice) strongly affects the diffractogram. We can observe a strong shift of the peak in the (111) direction, also see table S1. This peak is associated with a decrease of $\approx 5\%$ of the lattice parameter after the growth of 3 layers of CdS.

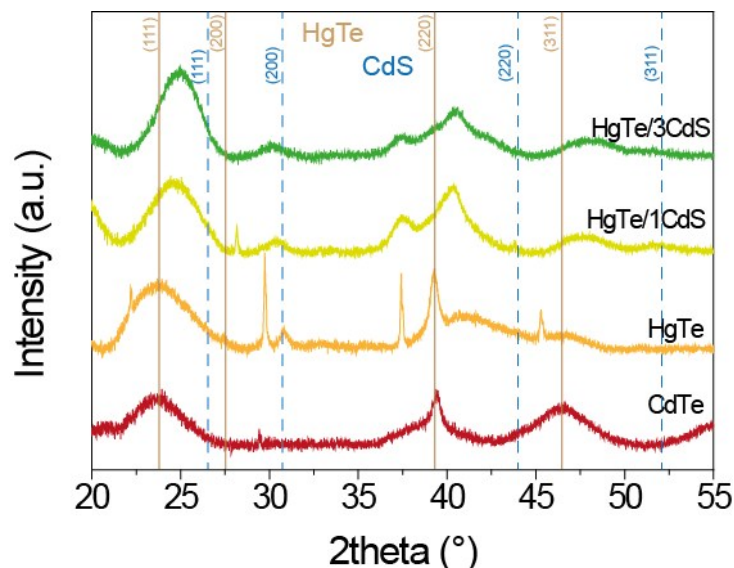


Figure S 3 X-ray diffractogram of CdTe, HgTe, HgTe/1CdS and HgTe/3CdS NPL

Table S1 diffraction angle associated with the (111) direction and lattice parameter for CdTe, HgTe, HgTe/1CdS and HgTe/3CdS NPL

Material	2 θ for (111) direction (°)	Lattice parameter (nm)
CdTe	23.56	0.653
HgTe	23.77	0.647
HgTe/1CdS	24.56	0.627
HgTe/3CdS	24.96	0.617

To achieve reasonably homogeneous thin film of NPLs we use a hexane:octane mixture with a 9:1 ratio in volume, see Figure S 4.



Figure S 4 Image of dropcasted solution of HgTe/CdS from hexane solvent and from hexane:octane mixture.

2. Photoemission signal

2.1. Core level analysis

Figure S 5 is the analysis of core levels from HgTe/3CdS. In particular, the Hg 4f state displays two contributions see Figure S 5b, similar to previous observations on mercury chalcogenide nanocrystals¹. The second contribution has been attributed to surface Hg. Regarding the Cd, there is only one main contribution, see Figure S 5c, appearing at a binding energy of 405.1 eV. The S 2p state reveals several components, see Figure S 5d. At least one is coming from the S from the shell and a second one from the thiol ligand (ethanedithiol) used to cap the NPLs during the photoemission measurements.

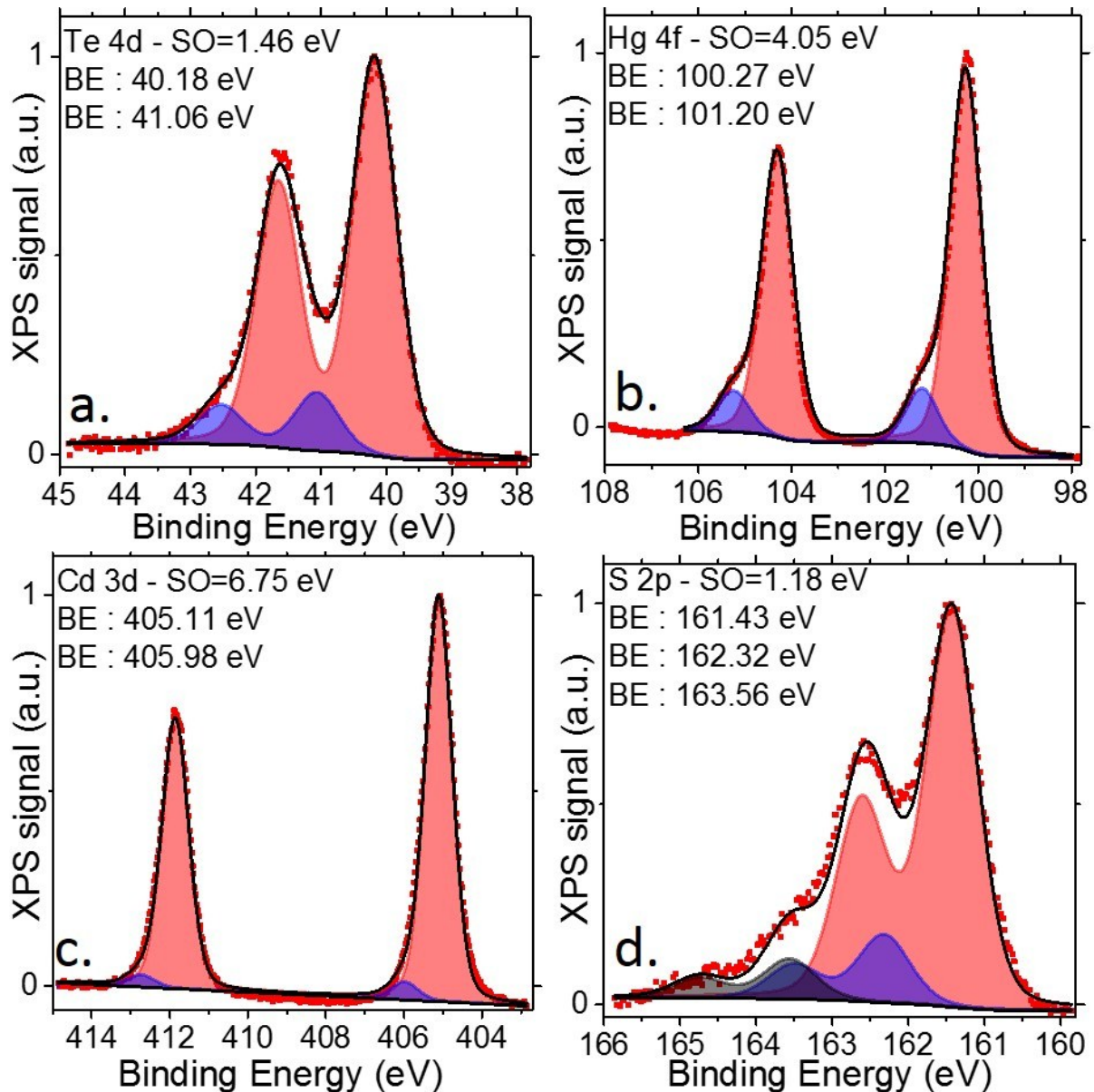
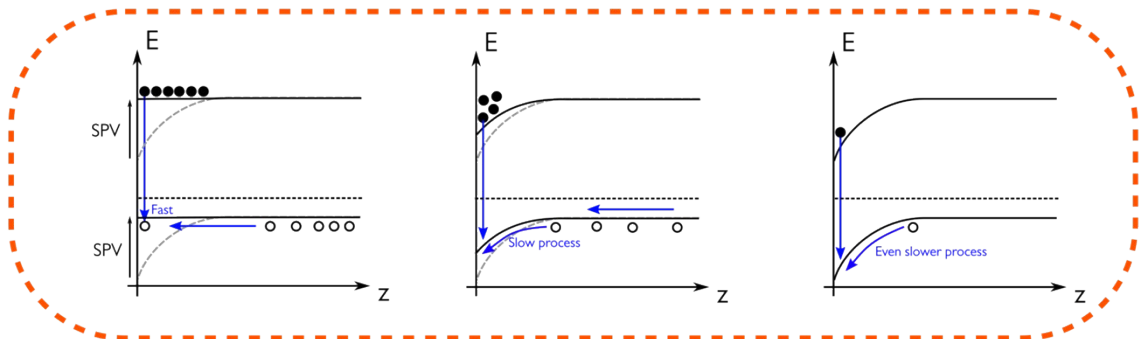
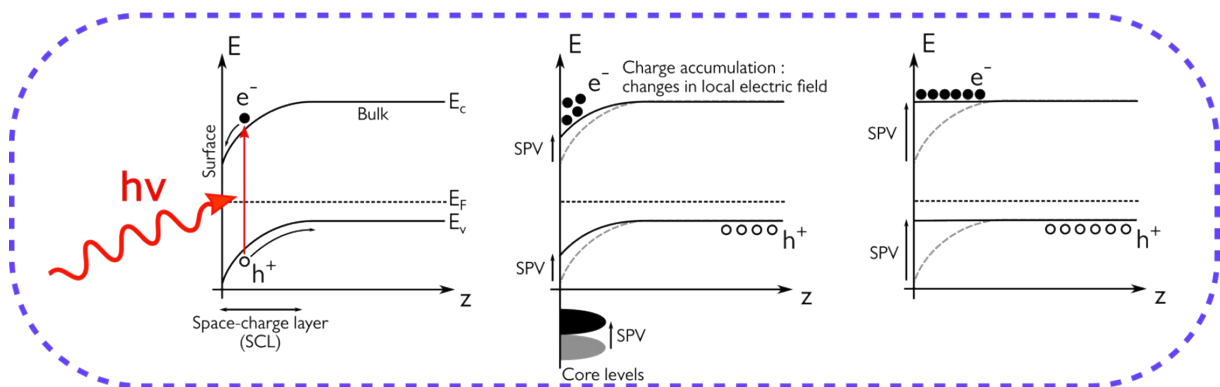


Figure S 5 Photoemission signal from a film of HgTe/3CdS NPLs associated with the Te 4d core level (a), Hg 4f core level (b), Cd 3d core level (c) and S 2p core level (d).

2.2. Pump probe photoemission

The time resolved photoemission is a surface photovoltage (SPV) measurement. It is used to determine the majority and minority carrier relaxation time. During the SPV measurements, the absorption occurs all over the semiconductor, but the SPV signal (shift in binding energy associated with a change of band bending) results from the contribution of the surface space charge region. In a doped semiconductor, the surface tends to be depleted and once photons are absorbed, excitons are generated. Due to the downward (resp upward) band bending occurring at the surface of a *p*-type (resp *n*-type) semiconductor, electrons and holes get split, and the minority carriers flow toward the surface until the establishment of a flat band (see *Figure S 6a*). The flow of the minority carriers is a self-decelerating process, since the driving force is the band bending and the latter is reduced by the process it-self, see top part of figure S. The turn-on time, which relates to the minority carriers has been measured in HgTe NPL to be in the 100-150 ns range. Here the illumination being an ultrashort pulse (<1ps) compare to the temporal resolution of the acquisition (30ns). The turn-on time can not be resolved

Laser ON : building-up SPV signal



Laser OFF : band-bending recovering

Figure S 6 Scheme of the surface photovoltage process in the case of a *p*-doped semiconductor such as the HgTe NPL capped with EDT, when the light is turned on (part a) and when the light is turned off (part b). Reprinted with permission from *Livache et al*². Copyright (2017) American Chemical Society.

As light is turned-off, the majority carriers flow from the bulk of the sample to refill the surface traps and restore the band bending, see bottom part of figure S. The turn-off time, which relates to the majority carrier transport, is in the 250 to 1000 ns range.

3. Experimental setup used for transport measurements

3.1. Field effect transistor measurements

DC transport. The sample is connected to a Keithley 2634b which controls the drain bias (V_{DS}) between -2 and +2 V with a step of 10 mV and measures the associated current (I_{DS}). This measurement is made in the dark and under illumination ($\lambda = 1.55 \mu\text{m}$).

Transistor measurements. The sample is connected to a Keithley 2634b which sets the drain bias ($V_{DS} = 0.1 \text{ V}$), controls the gate bias (V_{GS}) between -2 and +2 V with a step of 1 mV and measures the associated currents I_{DS} and I_{GS} . A scheme of the experimental setup is given in Figure S 7.

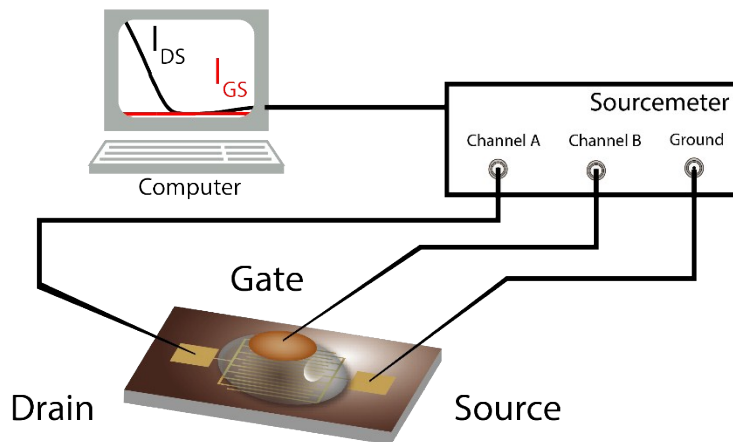


Figure S 7 Scheme of the setup used for field effect transistor measurements.

3.2. Time-resolved photoresponse

Time – resolved measurements: For the time-resolved measurements, we use a pulsed laser (Crylas FTSS 355-50) at 355 nm. The pulses are 1 ns long and repeated every 10 ms (100 Hz). A photodiode is used to trigger the signal. The bias, 50 V, is applied by a Keithley 2634b. An oscilloscope (Rohde & Schwarz, RTE 1102) acquires the outgoing signal through a 50Ω resistor, which is proportional to I_{DS} . The response of the film is measured at different time scales, normalized, and plot in a log-log plot. A scheme of the experimental setup is given in figure 5a.

Frequency resolved responsivity: to determine the response time of the HgTe/CdS NPLs in the short wave infrared, we bias the sample using a Keithley 2634b. The sample is illuminated using an electrically chopped laser diode at $1.55 \mu\text{m}$. The current is amplified using a current amplifier (Femto DLCPA 200) and the signal acquired on an oscilloscope (Tektronik TDC 5034). A scheme of the experimental setup is given in Figure S 8a. In the case of HgTe/3CdS, the Bode diagram of the responsivity is flat, see Figure S 8b, meaning that the dynamics of the device is beyond the capability of the setup (10 kHz).

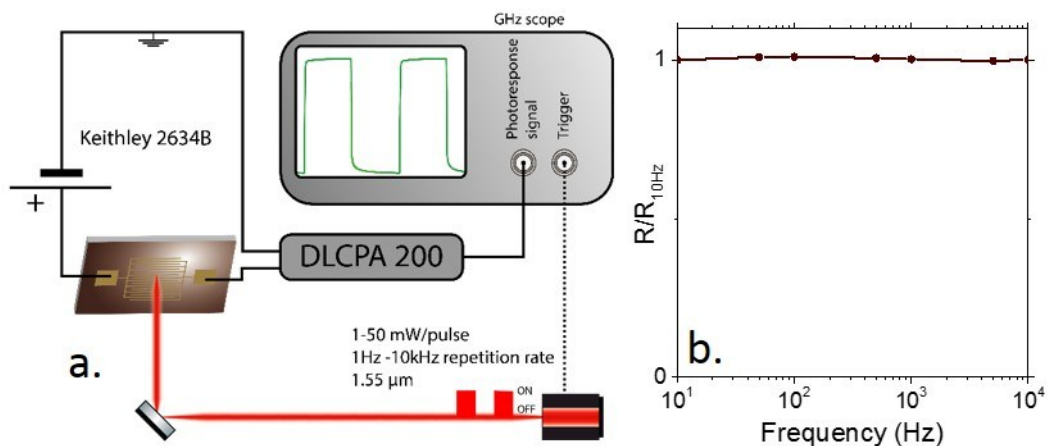


Figure S 8 a. Scheme of the setup used for time resolved photoresponse. b. Bode diagram of the photoresponse of HgTe/3CdS NPL film under excitation by a 1.55 μm laser.

3.3. Noise measurement

Noise measurements: To measure the noise, the sample is biased using a 1.5 V battery. The current through the sample is magnified using a Femto DLCPA 200 current amplifier. The current spectral density is acquired with a spectrum analyzer from Stanford instrument (SR 780). A scheme of the experimental setup is given in Figure S 9.

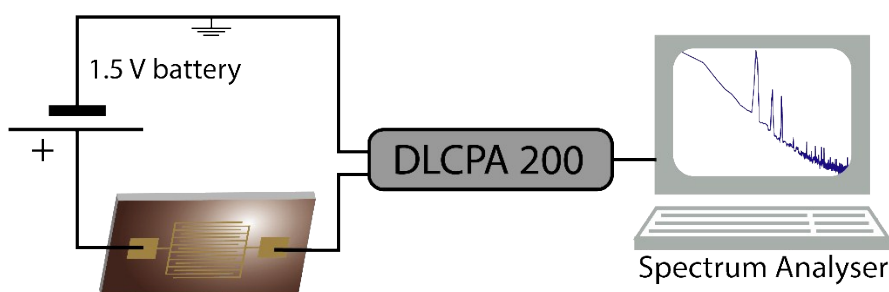


Figure S 9 Scheme of the setup used for the measurement of the noise spectral density.

4. References

- 1 B. Martinez, C. Livache, L. D. Notemgnou Mouafo, N. Goubet, S. Keuleyan, H. Cruguel, S. Ithurria, H. Aubin, A. Ouerghi, B. Doudin, E. Lacaze, B. Dubertret, M. G. Silly, R. P. S. M. Lobo, J. F. Dayen and E. Lhuillier, *ACS Appl. Mater. Interfaces*, 2017, **9**, 36173–36180.
- 2 C. Livache, E. Izquierdo, B. Martinez, M. Dufour, D. Pierucci, S. Keuleyan, H. Cruguel, L. Becerra, J. L. Fave, H. Aubin, A. Ouerghi, E. Lacaze, M. G. Silly, B. Dubertret, S. Ithurria and E. Lhuillier, *Nano Lett.*, 2017, **17**, 4067–4074.